ISBN 978-90-481-2483-1

NATO Science for Peace and Security Series - A:
Chemistry and Biology

Self-Organization of Molecular Systems

From Molecules and Clusters to Nanotubes and Proteins

Edited by
Nino Russo
Victor Ya. Antonchenko
Eugene Kryachko

Anharmonicity and Soliton-Mediated Transport: Thermal Solitons, Solectrons and Electric Transport in Nonlinear Conducting Lattices

W. Ebeling, M.G. Velarde, A.P. Chetverikov, and D. Hennig

Abstract We report here results about the excitation and survival of solitons in one-dimensional (1d) lattices with Morse interactions in a temperature range from low to physiological or room temperature (ca. 300 K). We also study their influence on added free electrons moving in the lattice. The lattice units (considered as "atoms" or "screened ion cores") are treated by classical (Newton–)Langevin equations. Then representing the densities of the core (valence) electrons of lattice units by Gaussian distributions we visualize lattice compressions as enhanced density regions. The local potentials created by the solitonic excitations are estimated as well as the classical and quantum–mechanical occupations. Further we consider the formation of solectrons, i.e. dynamic electron–soliton bound states. Finally, we add Coulomb repulsion and study its influence on solectrons. A discussion is also given about soliton-mediated electron pairing.

Keywords Morse interaction · Polaron · Soliton · Solectron · Electron pairing

1 Introduction

Excitation energy transfer processes in biological systems are problems of basic and long-standing interest [1–3], and especially the functional primary processes in photosynthetic reaction centers, drug metabolism, cell respiration, enzyme activities

W. Ebeling
Institut für Physik, Humboldt-Universität Berlin, Newtonstrasse 15, Berlin-12489, Germany
e-mail: ebeling@physik.hu-berlin.de

M.G. Velarde (✉)
Instituto Pluridisciplinar, Paseo Juan XIII, n. 1, Madrid-28040, Spain
e-mail: mgvelarde@pluri.ucm.es

A.P. Chetverikov
Dept. of Physics, Saratov State University, Astrakhanskaya 83, Saratov-410012, Russia
e-mail: chetverikovap@info.sgu.ru

D. Hennig
Institut für Physik, Humboldt-Universität Berlin, Newtonstrasse 15, Berlin-12489, Germany
e-mail: hennigd@physik.hu-berlin.de

N. Russo et al. (eds.), *Self-Organization of Molecular Systems: From Molecules and Clusters to Nanotubes and Proteins*, NATO Science for Peace and Security Series A: Chemistry and Biology,

and gene regulation have been studied intensively. In this context understanding the mechanism of electron transfer (ET) in biomolecules has attracted considerable attention during the last years [4–23]. The exploitation of the ET processes to construct technological devices has already been proposed and for such an achievement a theoretical understanding of the transfer mechanism in nature is needed and/or it has to be invented.

Inspired by the success of biomolecule modifications along with the determination of their three-dimensional structure microscopic theories for energy-transfer reactions were developed. Data of high resolving X-ray analysis gave the essential details on an atomic scale needed as input quantities for microscopic theories of ET in them. This gave insight into the relation between the structure and function for the energy and particle transfer in biomolecules and it has been shown how their steric structure can affect electron tunneling. In particular, experiments indicate that the H-bridges and covalent bonds involved in the biomolecules secondary structure are vital for mediating ET. On the other hand under physiological conditions (ca. 300 K) the ET may be activated by couplings to vibrational motion as long ago advocated by Hopfield [4]. Furthermore, molecular dynamics simulations have predicted that global molecule motions are very important for biochemical reactions for instance in light-induced reactions of chromophores accompanied by nuclear motions and for the ET in pigment protein complexes. In reaction center proteins proceed the protein nuclear motions coherently along the reaction coordinate on the picosecond time scale of ET as femtosecond spectroscopy revealed. Thus the vibrational dynamics of biomolecules may serve as the driving force of ET in them. Therefore investigations of transport mechanisms relying on the *mutual coupling between the electron amplitude and intramolecular bond vibrations* in biomolecules are of paramount importance.

Studies of energy storage and transport in macromolecules on the basis of self-trapped states have a long history beginning with the work of Landau [24] and Pekar [25, 26]. They introduced the concept of polaron (or as earlier said electron self-trapping), i.e. an electron accompanied by its own lattice distortion (a few phonons in another language) forming a localized quasiparticle compound which becomes the true electric carrier. In this context an approximate Hamiltonian system is often used to model transport of such localized excitations [27, 28]. When the size of the polaron is large enough so that the continuum approximation can be applied to the underlying lattice system in a clever combination of physical insight and mathematical beauty Davydov showed that a mobile self-trapped state can travel as a solitary wave along the molecular structure and he coined the concept of electro-soliton as electrical carrier and the natural generalization of the polaron concept [29–32]. Since the work of Davydov the relevance of solitons for the energy and particle transport in biomolecules has been recognized [33–36]. Similar ideas to Davydov's were also advanced by Fröhlich [37–43]; the relationship between the two approaches was elucidated in [44]. Most of the studies of transport properties in biopolymers are based on one-dimensional nonlinear lattice models, and recent two- and three-dimensional extensions with respect to solitonic transport of vibrational energy can be found, e.g. in [45–47]. Recent findings suggest that supersonic

acoustic solitons can capture and transfer self-trapping modes in anharmonic one-dimensional lattices [48]. Regarding the enforcing role played by soliton motion in the functional processes in biomolecules we note that recently it has been proposed that the folding and conformation process of proteins may be mediated by solitons traveling along the polypeptide chains while interacting with a field corresponding to the conformation angles of the protein [49]. Furthermore, in a nonlinear dynamics approach to DNA dynamics it has been suggested that solitons propagating along the DNA molecule may play an important role in the denaturation and transcription process [50–54].

Hence, for a theoretical understanding of ET mechanisms in biomolecule the models should not only incorporate the static aspect of the protein structure but also its dynamics [55]. In particular, it has been illustrated that the dynamical coupling of moving electrons to vibrational motions of the peptide matrix can lead to some biological reactions in an activationless fashion [56]. In this spirit the investigations in [57–65] have been devoted to bond-mediated biomolecule ET using the concept of breather solutions. The transfer of electrons along folded polypeptide chains arranged in three-dimensional conformations constituting the secondary helix structure of the proteins has been considered. It has been demonstrated that the coupling between the electron and the vibrations of the protein matrix can activate coherent ET.

In view of the above and to better place the work that follows here let us insist on the fact that it is the nonlinearity induced by the electron-(acoustic) phonon interaction that led Davydov to his electro-soliton concept for otherwise dynamically *harmonic* lattices. Davydov argued that these excitations could be stable at finite temperatures and could persist even at physiological or room temperatures. Several authors have checked this conjecture and have shown that Davydov's electro-solitons are destroyed already around 10 K lasting at most 2 ps [33–36]. We shall follow Davydov's line of thought here but rather than using a harmonic lattice we shall consider *anharmonic* lattice dynamics. It is now well established that if the underlying lattice dynamics involves *anharmonic* interaction this may result in the appearance of *supersonic* (acoustic) solitons running free along the lattice like in a Toda lattice and in some other cases [66–83]. We shall make use of the Morse potential [84] (akin to the Toda repulsive interaction and to the Lennard–Jones potential) together with the electron–(acoustic)soliton interaction. As shown in Fig. 1, these potentials can be scaled around the minimum in such a way that the first three derivatives are identical what guarantees a close relationship of their nonlinear (soliton) excitations when acting in a lattice. It is also known that these excitations bring a new form of dressed electrons or electro-soliton dynamic bound states [74–83]. They have been called solectrons to mark the difference with Davydov's electro-solitons (for further historical details see [85]). We shall show that due to the added lattice *anharmonicity* and the excitation of lattice solitons there is solectron stability well above 10 K, in fact up to the physiological or room temperature range (ca. 300 K).

After introducing the model lattice problem in Section 2, we develop in Section 3 a method of visualization of soliton excitations as well as estimation of their life

times. Discussed also there are the processes of solectron formation, electron pairing and solectron pair formation. In Section 4 using the tight-binding approximation we further explore how lattice deformations (or relative displacements between lattice units) affect solectron evolution. We also return there to the question of soliton-mediated electron pairing. In Section 5 we explore in depth how Coulomb repulsion affects solectron formation and electron pairing. A summary of results and comments are given in Section 6.

2 Lattice Dynamics

2.1 Lattice Anharmonicity and Temperature

We shall consider in a mixed classical–quantum description a 1d nonlinear lattice with added (free) conduction electrons allowing donor-acceptor electron transfer (ET) or electric current in the presence of an external field. The system consists of N classical units (atoms or screened ion cores). We shall focus on the case of periodic boundary conditions on a lattice like a ring of length L. These electrons are allowed to occupy some 3d volume surrounding the 1d lattice. For the *heavier* lattice units (relative to the electrons) we shall consider that have all equal mass m, and are described by coordinates $x_n(t)$ and velocities $v_n(t)$, $n = 1, \ldots, N$. We take

$$H_a = \frac{m}{2} \sum_n v_n^2 + \frac{1}{2} \sum_{n,j} V(x_n,\ x_j). \tag{1}$$

The subscripts locate lattice sites and the corresponding summations run from 1 to N. The mean equilibrium distance (lattice constant) between the particles in the lattice is σ ($\sigma = L/N$). We shall assume that the lattice particles repel each other with a strong Born repulsive force and attract each other with a weak dispersion force with a potential which depends on the relative distance $r = x_{n+1} - x_n$ between nearest-neighbors only. As earlier indicated we shall take the Morse function, one if not the earliest quantum-mechanics based interaction potential [84]. As Fig. 1 shows its repulsive core is to a good approximation like that of the Toda potential though the latter possesses an unphysical attractive component. As the Hamiltonian (Eq. (1)) with V taken as a Toda potential is integrable and we know analytically in compact form its exact solutions this is of interest to us as we shall be concerned with relatively strong lattice compressions where what really matters is atomic repulsion. On the other hand it also appears of interest that the Toda interaction yields the hard rod impulsive force in one limit (the fluid phase) while in another limit it becomes a harmonic oscillator (the solid lattice crystal-like phase). Thus we take

$$V = D\left\{\exp[2B(r-\sigma)] - 2\exp[-B(r-\sigma)]\right\}. \tag{2}$$

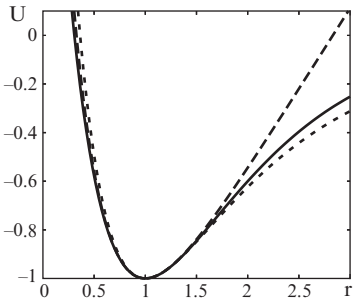

Fig. 1 Toda (*upper curve*), Morse (*middle curve*) and Lennard–Jones L-J(12-6) (*lower curve*) potentials suitably scaled around their minima to have identical second and third derivatives. Another L-J potential used by chemists is the so-called standard screw L-J(32-6) potential offering no added advantages for the purposes of this report

Exponentials are easily implemented in analog computers and they are also easier to handle mathematically for our purposes here. For illustration in our computer simulations we shall use $N = 200$ and $B = 1/\sigma$. B accounts for the stiffness along the lattice and D provides an estimate of the binding/break-up energy of lattice bonds.

Then in the presence of random forces (hence non zero temperature) and external forces, H, the evolution of lattice particles is described by the (Newton-)Langevin equations ($n = 1, 2, \ldots, N$) [86]

$$\frac{d v_n}{dt} + \frac{1}{m}\frac{\partial H}{\partial x_n} = -\gamma_0 v_n + \sqrt{2D_v}\,\xi_n(t), \tag{3}$$

where the stochastic force $\sqrt{2D_v}\,\xi_n(t)$ models a surrounding heat bath (Gaussian white noise). The parameter γ_0 describes the common standard friction frequency acting on the lattice units or atoms from the surrounding heat bath. The validity of an Einstein relation is assumed $D_v = k_B T \gamma_0/m$, thus binging temperature T; k_B in Boltzmann's constant. In most cases we shall use σ as the length unit (though in occasions we may use $1/B$) and the frequency of oscillations around the potential minimum ω_0^{-1} as the time unit. Typical parameter values for biomolecules are $\sigma \simeq 1 - 5\mathring{A}$; $B \simeq 1\mathring{A}^{-1}$; $D \simeq 0.1 - 0.5$ eV [87–89]. This means that $B\sigma \simeq 1$ (it could take a higher value) and $1/\omega_0 \simeq 0.1 - 0.5ps$. As the energy unit we shall use $2D = m\omega_0^2\sigma^2/(B\sigma)^2$, that with $B\sigma = 1$ reduces to $m\omega_0^2\sigma^2$, commonly used by most authors. This energy will be used also as the unit to measure the temperature T ($k_B = 8.6 \cdot 10^{-5}\mathrm{eV}/K$; $k_B T = 2D$).

The specific heat (at constant volume/length) of system Eqs. (1)–(3) is shown in Fig. 2. Accordingly, the region where *anharmonicity* plays significant role is $0.75 < C_v/k_B < 0.95$. This is the multiphonon range or highly deformed-phonons domain on the way to melting in the system (recall that at high T, $C_v = 0.5$, there is transition to a hard-sphere fluid phase). The corresponding temperatures in our energy units are in the range $T \simeq 0.1$–0.5 (and even up to 1–2). Introducing the binding strength of the Morse lattice, as the Morse potential can be suitably adapted to the Toda interaction (Fig. 1), we foresee that solitonic effects are to be

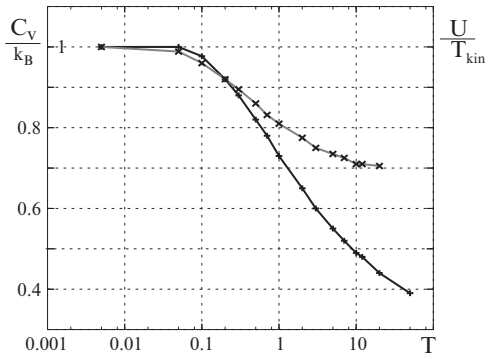

Fig. 2 Toda–Morse lattice. Specific heat at constant volume/length (*upper curve*) and ratio of *potential* energy, U, to *kinetic* energy, T_{kin} of the anharmonic lattice. Note that we have only the "high" temperature range

expected in the range $T_{sol}^{M} \simeq 0.2 - 1.0D$. In electron volts this would be the range $T_{sol}^{M} \simeq 0.01 - 0.1$ eV. This range of temperatures includes for biomolecules the range of physiological temperatures (ca. 300 K).

2.2 Lattice Units as Atoms and Lattice Solitons

We can visualize the time evolution of the lattice atoms and hence the lattice deformations or lattice excitations by representing the density of the *valence* electrons which are moving bound to the ion cores. This can be achieved by considering, for simplicity, that each lattice unit is surrounded by a Gaussian electron density (atomic density) of width, e.g. $s = 0.35\sigma$. Then the total atomic electron density is given by

$$\rho(x) = \sum_{n} \frac{1}{\sqrt{2\pi}s} \exp\left[-\frac{(x - x_n(t))^2}{2s^2}\right]. \tag{4}$$

Thus each lattice atom is like a spherical unit with continuous (valence) electron density concentrated around its center. In regions where the atoms overlap, the density is enhanced. This permits identifying solitonic excitations based on a color code in a density plot. This is of course a rough approximation which helps visualization of the location of dynamic excitations by using the (covalence) electrons density enhancements as an alternative to directly locating mechanical lattice compressions. For our purposes in Sections 2 and 3 this suffices. The mechanical approach is used in Sections 4 and 5. We show in Fig. 3 the results of computer simulations for three temperatures $T = 0.005$ ($\sim$10 K), $T = 0.1$ ($\sim 2 \cdot 10^2$K) and $T = 0.5$ ($\sim 10^3$K) with $D = 0.1$ eV. If we use $D = 0.05$ eV, then $T = 0.5$ corresponds to $T = 575$ K.

The diagonal stripes correspond to regions of enhanced density which are freely running along the lattice, this is the sign of solitonic excitations. Checking the slope we see that the excitations which survive more than 10 time units move with *supersonic* velocity. The pictures shown are quite similar to those described by Lomdahl and Kerr [33, 36] who gave a life-time of at most 2 ps and being stable

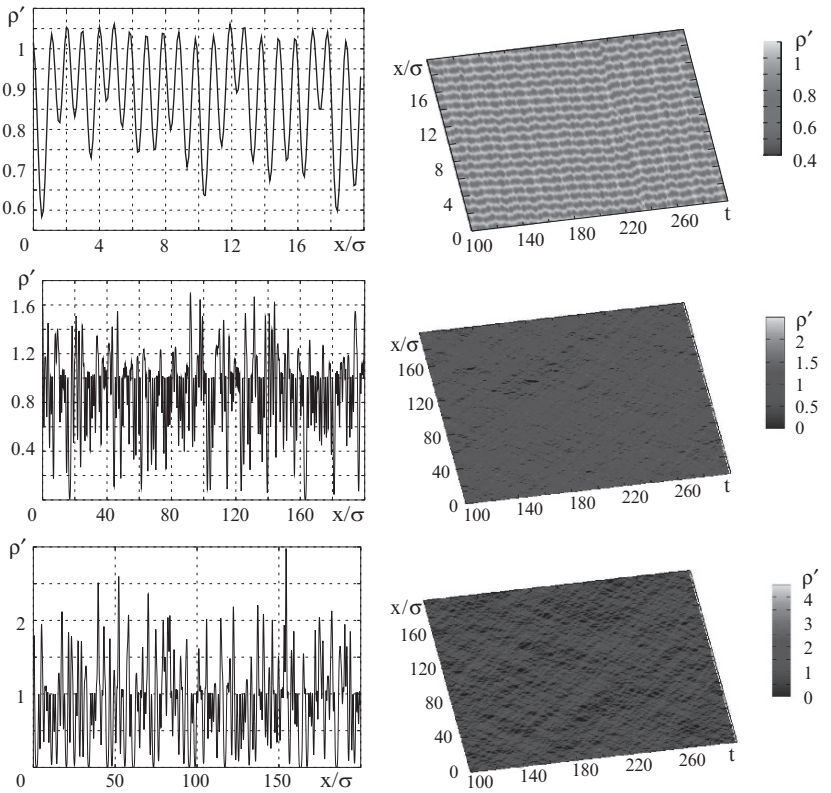

Fig. 3 Toda–Morse lattice. Visualization of running excitations (phonons and solitons) along the lattice. For convenience we use $\rho' = \sqrt{2\pi}s\rho$ to account for atomic core (valence) electrons density (the grey scale coding is in arbitrary units). We study three temperatures (given in units of $2D$): upper set of figures: $T = 0.005(\sim 10\,\mathrm{K})$: we see only harmonic lattice vibrations or phonons and no evidence of strong (soliton-like) excitations; center two-figures: $T = 0.1(\sim 2.10^2\,\mathrm{K})$: many density peaks show solitons (diagonal stripes). The strongest compressions move with velocity around $1.1v_{sound}$; lower two-figures: $T = 0.5(\sim 10^3\,\mathrm{K})$: among the many excitations appearing we observe solitons running with velocity around $1.3v_{sound}$. Parameter values: $N = 200$ and $B\sigma = 1$

only up to 10 K. Ours, however, live about 10–50 time units that is for several picoseconds and survive even at $T = 1$ which is well above physiological temperatures. This confirms an earlier finding were at $T \simeq 300$ K stable solitons and solectrons could be identified [79, 80]. Recall that Davydov's electro-solitons and hence Lomdahl and Kerr's earlier mentioned work refer to solitons induced by the presence of originally free (conduction) electrons and subsequent electron–phonon (polaron-like states) whereas in the case described in this Section the conduction electrons are yet to be added as we shall do in the following section.

3 Local Electronic States

Let us now add to the system free electrons surrounding in 3d space the 1d lattice (Fig. 4).

3.1 Local Pseudo-Potentials and Classical Densities

The lattice creates a field which acts on the free electrons. In order to construct this field we need to evaluate the interaction between the lattice units and the surrounding electrons. The latter form a narrow 3d neighborhood of the lattice with diameter about the Bohr-radius a_B.

We can assume that all lattice atoms (with their valence electrons) which are near to each other by 1.5σ or less contribute to the local potential $V(x)$ acting on each conduction electron

$$V(x) = \sum_n V_n(x - x_n), \qquad r = |x - x_n| < 1.5\sigma. \tag{5}$$

The potential $V_n(x - x_n)$ created by the lattice particles n at the place of the electron x may be estimated by a pseudo-potential approach [90, 91]. One possible ansatz for the interaction of electrons with ions is

$$V_n(y) = -U_e \frac{h}{\sqrt{y^2 + h^2}}. \tag{6}$$

The value of the binding energy U_e is in the range $U_e \simeq 0.05 - 0.1$ eV. This is a second (independent) energy unit of the system, in general lower in value than the earlier mentioned binding energy between lattice units. Let us consider for numerical convenience $U_e \simeq 0.02 - 0.2D$ and $h = 0.3\sigma$. The choice $h = 0.3\sigma$ provides shallow minima at the location of the lattice atoms with significantly deep local minima at the location of lattice compressions. In view of the value U_e the electrons are only weakly bound to the atoms and may transit from one side to the other of a lattice unit. Accordingly the (free) conduction electrons are able to wander through the lattice eventually creating an electron current. To place a pair of such electrons between two lattice particles is in general not favorable in energetic terms, since the energy of repulsion $e^2/\varepsilon_0 r$ has to be overcome; ε_0 denotes dielectric constant. However the electron may bind to more than two lattice atoms thus forming a deep potential hole akin to a *polaron* state which is a *static* structure corresponding to

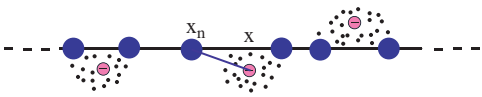

Fig. 4 Toda–Morse lattice. Sketch of lattice atoms or ion cores surrounded by added free electrons in 3d space

favorable energetic configurations. Here we are rather interested in the *dynamic* or time evolving phenomena initiated by solitonic excitations in the lattice. However we have to take into account that both of these items, the local compression by a static process (polaron formation) and by a running compression (soliton excitation) are intimately connected.

In the simplest entirely classical approximation we can assume that the evolution of the conduction electrons is very fast and the corresponding probability density follows locally a Boltzmann distribution. Note that when the electron density is sufficiently low, so that the electrons are still nondegenerated we may approximate the Fermi statistics by the Boltzmann statistics. In a heated lattice the units perform quite complex motions, we may expect therefore a rather complex structure of the field acting on the electrons. Let us give now examples of the fields created by the lattice atoms. The potential energy is given in units of the binding energy U_e. Taking into account the energy unit $2D(B\sigma)^2$ $(= m\omega_0^2\sigma^2)$, the scale is set by the ratio $\eta = \frac{U_e}{2DB^2\sigma^2} = \frac{1}{2B^2\sigma^2}\frac{U_e}{D}$. For $B\sigma = 1$ the energy scale is therefore $\eta = \frac{U_e}{2D}$. To estimate any physical quantity the value of η is very important.

The potential $V(x,t)$ is time-dependent and gives at each time instant a snapshot of the actual situation. The potential changes quickly and the distribution of the electrons tries to follow it as fast as possible and hence the electrons are "slaved" accordingly, thus permitting an *adiabatic* approximation. We have a situation similar to that described for free electron statistics in semiconductor theory [92]. Then, we assume as a first approximation a Boltzmann distribution

$$n(x,t) = \frac{\exp[-\beta V(x,t)]}{\int dx' \exp[-\beta V(x',t)]}, \tag{7}$$

with $\beta = 1/k_B T$. Here x denotes the coordinate along the lattice. An example of the estimated density Eq. (26) is shown in Fig. 5. The (relatively high) peaks correspond to the enhanced probability of a rather strong lattice compression, i.e., a soliton ready to meet and trap an electron. This defines the solectron as an electron "surfing" on a soliton for about 10–50 time units (i.e. a few picoseconds) then getting off it and eventually finding another soliton partner once more to surf-on and so on. For $T = 0.1$ we observe several rather stable running excitations (diagonal stripes) with velocities around $1.2v_{sound}$. For $T = 1$ (not shown in the figure) one can observe many weak and only a few very stable excitations moving with *supersonic* velocity $1.4v_{sound}$. The probabilities estimated from the Boltzmann distribution are strongly concentrated at the places of minima. This means that most of the electrons are concentrated near to solitonic compressions.

3.2 Bound States of 3d Electrons in a Nonlinear Lattice Ring

So far our estimates of the electronic states in the local potential were entirely classical. The Boltzmann distribution finds the deepest minima of the local potential

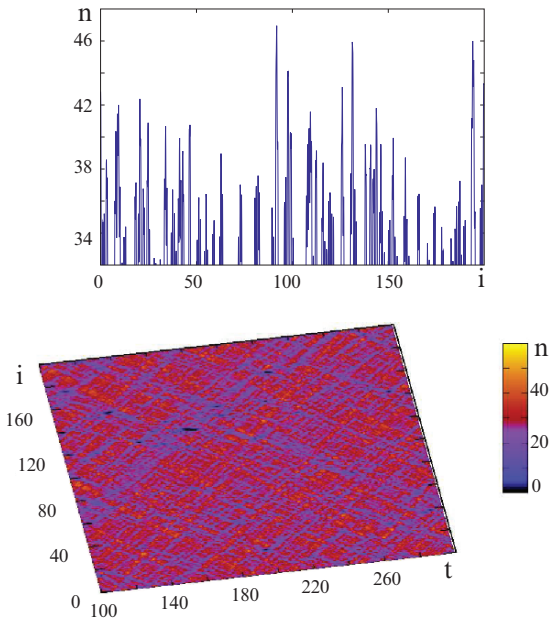

Fig. 5 Heated Toda–Morse lattice. Classical probability distribution of an electron in a heated anharmonic lattice in the *adiabatic* approximation according to local Boltzmann distribution. On the upper figure a snapshot of the distribution is given for a certain time instant. On the lower figure the actual time evolution of the distribution is displayed. The temperature is $T = 0.1$. Parameter values: $N = 200$, $h = 0.3$, $\sigma = 1$ and $B\sigma = 1$

$V(x,t)$ acting on an electron. The problem to find the quantum states for an electron in the anharmonic lattice is more difficult. There exist different situations depending on the relative values of the four length scales a_B, h, σ, d, where a_B is Bohr-radius, h is kind of softness scale of lattice particles (according to the pseudopotential (Eq. (6)), σ is the lattice spacing at equilibrium and d is the smallest interatomic lattice distance at solitonic compressions. As earlier noted, the character of the electron dynamics depends strongly on the value of h and on the distance σ. Figure 6 shows that the choice $h = 0.3\sigma$ depending on the distance between the neighbors in the lattice allows two kinds of minima. Accordingly, for a compressed lattice with $a_B \simeq h \simeq \sigma$ and $d < \sigma$, solectrons are to be expected.

Let us investigate now the conditions for possible formation of pairs of solectrons and under which conditions a solectron pair is more stable than a single solectron. As shown above, the electrons in soliton-bearing lattices move in a fastly changing potential landscape. The structure of this landscape is similar to the landscapes known from the theory of disordered systems [93–95]. At variance with the latter cases, our potential is time-dependent. In typical snapshots of the potential landscape acting on the electrons we see relatively flat normal parts showing only small oscillations of the potential and deep local minima which move approximately with soliton velocity. Certainly, the character of the bound states which may be formed depends on the depth of the potential U_{min}, on the temperature T and on the relation

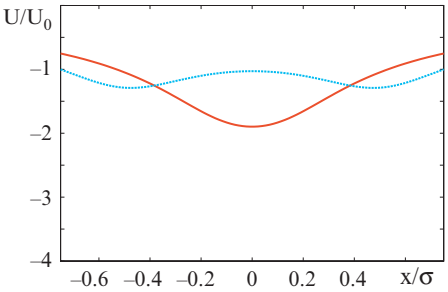

Fig. 6 Potential (in units of U_0) felt by an electron placed between two ions *versus* lattice spacing. If the ions are at equilibrium distance $r = \sigma$ the potential minima are at the center of two nearby ion cores. Between two compressed ions $r = \sigma/5$, a new potential minimum appears midway between two nearest-neighbor ions

between the characteristic quantum time $\tau_q \propto \hbar/U_{min}$ and the classical time scale $1/\omega_0$. Assuming that the classical time scale is much longer, we may work in an adiabatic approximation. Let the deep potential minimum (like a potential well) created by a soliton be approximated by a parabolic profile

$$U(r) = U_0 + \frac{a_0}{2} r^2 + ... \tag{8}$$

where r denotes distance in 3d space. The second derivative is

$$a_0 = U''(r)|_{r=r_0} \simeq \frac{c}{\sigma^2}, \tag{9}$$

with $c \simeq 1$. A typical valley includes just a few lattice units. Then the bound states are approximately given by

$$\varepsilon_n = U_0 + 3\hbar\omega_0 \left(n + \frac{1}{2} \right), \qquad n = 0, 1, 2, \ldots \tag{10}$$

where $a = m\omega_0^2$. The ground state wave function is

$$\Psi_0(r) = (r_0)^{-3/2} \pi^{-3/4} \exp(-r^2/2r_0^2), \tag{11}$$

where $r_0^2 = (\hbar/m\omega_0)$. Note that this estimate is valid only for sufficiently deep minima. These states can in principle be filled by electrons albeit obeying Pauli's exclusion principle. In the ground state, if sufficient solitons are available, each of the solitons can capture two electrons with opposite spin or possibly more electrons as suggested by classical estimates. However higher occupation is less probable. Indeed a second electron with opposite spin may be placed on the same level as the first one, but a third electron in a potential valley cannot occupy the ground state level any more.

3.3 Binding Energy and Wave Functions of Solectron Pairs

As we have seen, the potential well created by a soliton may in principle be occupied by pairs of electrons with opposite spins satisfying Pauli's exclusion principle. At first sight, these electron pairs, which are Bosons, appear like "bipolarons" or "Cooper pairs". However looking at the details we see, that the solectron pairs are something new. The problem of pairs or clusters of quantum electrons in a parabolic trap is not new [96–98]. In the case of solectrons the width of the potential well is of the order of a few equilibrium inter-atomic lattice distances. In a first estimate the energy of a solectron is about

$$\varepsilon_n = U_0 + \frac{3}{2}\hbar\omega_{min}, \tag{12}$$

and correspondingly the ground state energy of a Coulomb pair is

$$\varepsilon_{0p} = 2\Big[U_0 + \frac{3}{2}\hbar\omega_0\Big] + \langle\frac{e^2}{\varepsilon_0 r_p}\rangle, \tag{13}$$

where r_p is the distance of the electrons in the pair and as earlier ε_0 is the dielectric constant of the medium. Due to the factor two this energy is in general lower than the energy of the state of one bound and one free electron. If the term arising from Coulomb repulsion is weak, pairing is favorable. An estimate follows from the condition that repulsion and attraction to the center of the well balance each other

$$m\omega_0^2 r_1 = \frac{e^2}{\varepsilon_0(2r_1)^2}. \tag{14}$$

This leads to a classical estimate of the Coulomb shift

$$\Delta\varepsilon_{cl} = \frac{e^2}{2\varepsilon_0 r_1} = \left[\frac{e^2}{\varepsilon_0}\right]^{2/3}(m\omega_0^2)^{1/3}. \tag{15}$$

Within quantum theory we may estimate the Coulomb shift by using perturbation theory as done in the study of the Helium atom. We take two electrons which are confined in the field of a spherical potential well given by Eq. (8). The symmetric ground state wave function of two electrons with opposite spin is given by

$$\Psi(r_1, r_2) = \frac{1}{\pi^3 r_0^6}\exp\left[-\frac{r_1^2 + r_2^2}{2r_0^2}\right]. \tag{16}$$

The mean energy calculated with these wave functions is then

$$\varepsilon_{p0} = 2U_0 + 3\alpha\hbar\omega_0 + \Delta\varepsilon_{qm}, \tag{17}$$

$$\Delta\varepsilon_{qm} = \frac{1}{\pi r_0^6}\int dr_1 \int dr_2 \frac{e^2}{\varepsilon_0 |r_1 - r_2|} \exp\left[-\frac{r_1^2 + r_2^2}{2r_0^2}\right]. \tag{18}$$

After doing the integral over the angles (Eq. (18)) becomes

$$\Delta\varepsilon_{qm} = \frac{16e^2}{\pi r_0^6}\int_0^\infty dr_1 r_1 \exp[-r_1^2/r_0^2] \int_0^{r_1} dr_2 r_2^2 \exp[-r_2^2/r_0^2], \tag{19}$$

or else

$$\Delta\varepsilon_{qm} = \frac{e^2}{\varepsilon_0 r_0} A_0, \tag{20}$$

where the constant is defined by the integral

$$A_0 = \frac{16}{\pi}\int_0^\infty dy y \exp[-y^2] \int_0^y dz z^2 \exp[-z^2] \approx 0.32. \tag{21}$$

In view of this estimate, the mean distance between the electrons in a solectron pair is around $3r_0$, i.e. three times the "size" of the wave function. We expect that the real Coulomb shift is between the classical and the quantum estimates. In order to find solectron pairs we need conditions where the Coulomb shift is much smaller than the gap to the next level which is $3\,\hbar\omega_0$. To be on the safe side we require conditions such that

$$max[\Delta\varepsilon_{cl}, \Delta\varepsilon_{qm}] < 3\hbar\omega_0. \tag{22}$$

Under these conditions the formation of a solectron pair is favored.

3.4 Soliton Mediated Electron Pairing

Let us further comment on how electron pairing could be influenced by the presence of solitons. If one could obtain Boson pairs with sufficient density, then interesting effects may be expected. Looking at the classical probability distributions in Figs. 3 and 5 we see that there are minima of different types. There are flat and narrow minima which carry just one electron as in a solectron. Further there are minima with two electrons and finally deep minima capable of carrying many electrons. In fact as Figs. 3 and 5 show most of the minima carry 3–10 electrons. However quantum-mechanical effects rather provide a new picture: (i) quantum solectrons are in energy just a bit higher than the classical solectrons due to the ground state energy shift $1.5\hbar\omega_0$; (ii) a second electron with opposite spin may be placed at the

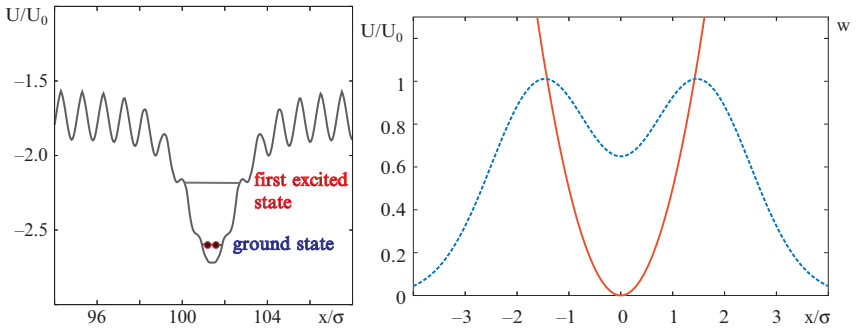

Fig. 7 Toda–Morse lattice. Left figure: formation of an electron pair in the potential minimum created by a solitonic excitation in the lattice. The formation of a trio requires a much higher energy. Therefore a solectron trio is ruled out except at very high temperatures. Right figure: shape of the pair wave function near to the minimum of the potential

same level (see Fig. 7). These solectron pairs are rather stable since the binding of a third electron needs a relatively high amount of energy, namely $3\hbar\omega_0$.

Let us estimate the chance to form trios. To place another electron into a solitonic well which is already occupied by an electron-pair needs the overcoming of a gap with the amount $3\hbar\omega_0$ between the ground state and the first excited level. Thus if

$$k_B T < 3\hbar\omega_0, \tag{23}$$

the occupation by trios, quartets, etc. (which is classically possible) is more or less prevented by quantum effects. Indeed we may assume that the extension of a solitonic minimum is about ten times wider than the Morse potential minimum (Fig. 1). Such minimum corresponds to a frequency about $3 \cdot 10^{12}\mathrm{s}^{-1}$. Then the frequency of oscillations around the minimum of the soliton potential is about $10^{12}\mathrm{s}^{-1}$. This is about $1 - 2$ eV. Accordingly, the inequality (Eq. (23)) implies $T < 10^3\mathrm{K}$ naturally fulfilled in all interesting cases.

Thus under special conditions, in certain windows of parameter values, the formation of pairs is more favorable than the single solectron. Under quasi-classical conditions however the system seems to favor electron clusters. In conclusion we may say that the Pauli exclusion principle has the consequence that instead of classical clusters we observe quantum–mechanical pairs of solectrons. This supports the soliton-mediated electron pairing mechanism proposed by Velarde and Neissner [99] (Fig. 8).

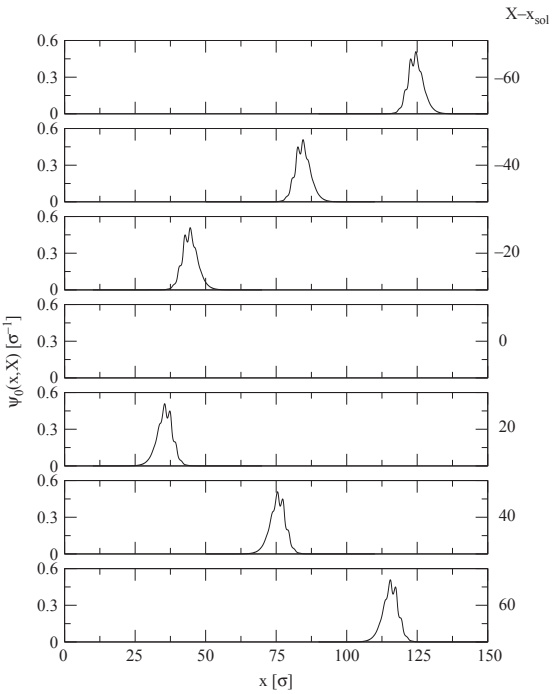

Fig. 8 Toda–Morse lattice. Evolution of the wave function of an electron-electron pair created by a moving solitonic lattice deformation [99]

4 Electron-Lattice Dynamics in Tight-Binding Approximation

Let us now go deeper into the question of solectron formation by describing the electrons on the lattice using the tight-binding approximation (TBA).

4.1 The Tight-Binding Approximation

The tight-binding approximation replaces the Schrödinger continuum dynamics by a hopping process along the discrete lattice sites. Assuming that there is only one atomic state per lattice unit we get for the electrons the following Hamiltonian in second-quantization formalism [100, 101]

$$H_{el} = \sum_n \big[E_n(..., x_{n-1}, x_n, x_{n+1}, ...) c_n^+ c_n - V_{n,n-1}(x_n, x_{n-1})(c_n^+ c_{n-1} + c_n c_{n-1}^+) \big] . \quad (24)$$

Recall that (24) refers to initially *free* or *excess* electrons added to the lattice with atoms assumed to be located at sites n. The quantities c_n, c_n^+ originally refer to Fermion destruction and creation operators, respectively, with appropriate anti-commutation relations but here they are just complex numbers. Purposedly in this section we shall consider the non-uniformity of the on-site energy levels (diagonal elements, V_{nn}, of the transfer matrix). Further assuming that the interaction depends exponentially on the distance between the lattice units, we set

$$V_{n,n-1} = -V_0 \exp[-\alpha(q_n - q_{n-1})]. \tag{25}$$

Then the Hamiltonian (Eq. (24)) becomes

$$H_{el} = \sum_n \left\{ (E_n^0 + \delta E_n) c_n^+ c_n - V_0 \exp[-\alpha(q_n - q_{n-1})](c_n^+ c_{n-1} + c_n c_{n-1}^+) \right\}, \tag{26}$$

where, for convenience in notation, q_n denotes a lattice site spatial vibration (relative displacement) coordinate defined by $x_n = n\sigma + q_n/B$. The term E_n^0 denotes on-site energy levels of the unperturbed lattice and δE_n is the perturbation due to the lattice vibrations (harmonic as well as anharmonic modes may contribute). The simplest approximation is

$$\delta E_n = \chi(q_n/B), \tag{27}$$

where the "electron–phonon coupling constant", χ, indicates that the on-site energy level E_n, i.e. the local site energy, depends on the displacement of the unit at that site; q_n is dimensionless (unit: $1/B$). As shown e.g. in [87–89], this coupling between lattice deformations and electronic states, leads for large enough values of the parameter χ to the formation of *polarons*. In view of the above given parameter values, the value of the coupling constant is in the range $\chi \simeq 0.1 - 2$ eV/Å. We have to take into account that our model is translationally invariant and we are considering relative lattice displacements. Accordingly, we set

$$\delta E_n \simeq \frac{\chi_1}{2} \left[(q_{n+1} - q_n) + (q_n - q_{n-1}) \right], \tag{28}$$

with $\chi_1 = \chi/B$ as a new constant. An alternative, using a pseudopotential like Eq. (6), is the approximation

$$E_n = E_n^0 - U_e \sum_{j \neq n}{}' \frac{h}{\sqrt{(x_n - x_j)^2 + h^2}}, \tag{29}$$

where the over-dash in the sum indicates that it is to be restricted in an appropriate way by introducing screening effects. For instance, as earlier done, we may cut the sum at a distance 1.5σ from the center of the ion core, or in other words include all terms corresponding to lattice units which are nearer than 1.5σ. Then we assume that the energy levels are shifted like the field created by the pseudopotentials acting

on the electron from the side of the neighboring atoms. To linear approximation we get

$$\delta E_n \simeq \frac{hU_e\sigma}{B(\sigma^2+h^2)^{3/2}}\left[(q_{n+1}-q_n)+(q_n-q_{n-1})\right]. \tag{30}$$

Comparing Eqs. (28) and (30) we find

$$\chi = U_e\frac{2\sigma h}{(\sigma^2+h^2)^{3/2}} = \left(\frac{U_e}{\sigma}\right)\frac{2(h/\sigma)}{[1+(h/\sigma)^2]^{3/2}}. \tag{31}$$

Then for $U_e = 0.1-1.0D$, $h = 0.3\sigma$, $D = 0.1-0.5$ eV, and $\sigma = 1-5$Å we obtain $\chi = 0.001-0.1$ eV/Å. As the parameter values in this approach are about one or two orders of magnitude below the earlier indicated values we expect that here polaron effects are rather weak and hence the system dynamics is dominated by solitons.

The probability to find the electron at the lattice site or atom located at x_n, i.e. the occupation number p_n, is $p_n = c_n c_n^*$. Solving the Schrödinger equation for the components of the wave function c_n we get

$$\begin{aligned} i\frac{dc_n}{dt} &= \tau[E_n^0+\delta E_n(q_{n+1},q_{n-1})]c_n \\ &\quad -\tau\left\{\exp[-\alpha(q_{n+1}-q_n)]c_{n+1}\right. \\ &\quad \left.+\exp[-\alpha(q_n-q_{n-1})]c_{n-1}\right\}, \end{aligned} \tag{32}$$

where E_n^0 and δE_n are dimensionless (unit: 2D). The corresponding Newtonian equations for the lattice units are

$$\begin{aligned} \frac{d^2q_n}{dt^2} &= -p_n\frac{\partial\delta E_n(q_{n+1},q_{n-1})}{\partial q_n} \\ &\quad +\{1-\exp[-(q_{n+1}-q_n)]\}\exp[-(q_{n+1}-q_n)] \\ &\quad -\{1-\exp[-(q_n-q_{n-1})]\}\exp[-(q_n-q_{n-1})] \\ &\quad -\alpha V_0\left\{\exp[-\alpha(q_n-q_{n-1})](c_{n+1}^+c_n+c_{n+1}c_n^+)\right. \\ &\quad \left.+\exp[-\alpha(q_{n+1}-q_n)](c_n^+c_{n-1}+c_nc_{n-1}^+)\right\}. \end{aligned} \tag{33}$$

The role of temperature would be considered further below. The problem reduces, in principle, to solving both Eqs. (32) and (33) coupled together. It is not, however, the only possible approach to our problem as we shall see below.

4.2 *Discussion About Solectronic Excitations and Expected Consequences*

Let us consider one of the possible soliton-mediated processes: single electron transfer (ET) in a soliton-mediated hopping process along the lattice from a *donor* to an *acceptor*. When an added, excess electron is placed at a *donor* located at site

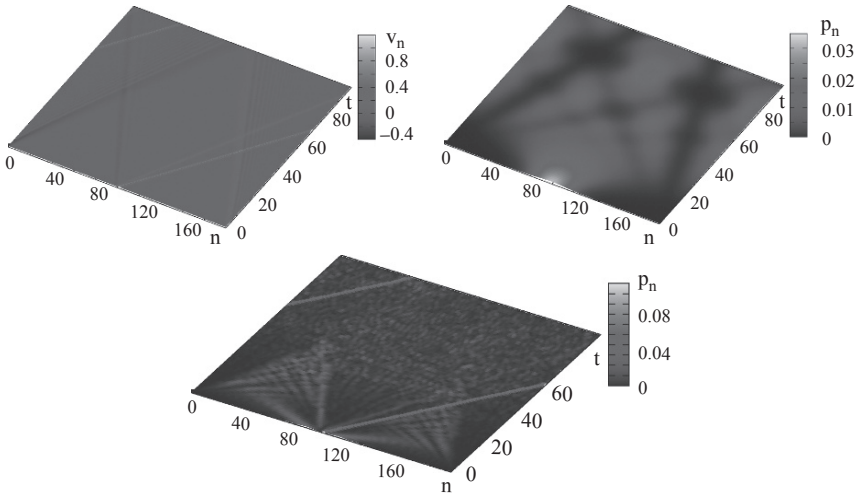

Fig. 9 Toda–Morse lattice. Soliton, electron and solectron. Results of numerical integration of Eqs. (32) and (33). Upper left figure: $\alpha = 0$, soliton alone; upper right figure: $\alpha = 0$, electron alone; bottom figure: $\alpha = 1,75$, solectron (electron dynamically bound to the soliton). The grey scales (velocity and probability density) are in arbitrary units, just for illustration

$n = 100$ at time $t = 0$, Fig. 9 shows our findings: (a) pure anharmonic lattice vibration without electron–lattice interaction ($\alpha = 0$): time evolution of one soliton as predicted by the Morse Hamiltonian (Eq. (33)), thus illustrating how little we depart from the Toda solitons; (b) free electron alien to lattice vibrations ($\alpha = 0$): spreading of the free electron probability density as a consequence of Schrödinger equation (32); and (c) electron-lattice interaction ($\alpha = 1,75$): soliton-mediated ET as predicted by Eqs. (32) and (33) coupled together. The electron is dynamically bound to the soliton which is the solectron excitation.

When the electron–lattice interaction is operating, we see that the electron moves with the soliton with a slightly supersonic velocity $v_{el} \sim \frac{100}{70} v_{sound}$ and is running to the right border of the square plot. Let us assume that there an acceptor is located. This means that the electron is guided by the soliton from *donor* to *acceptor*. In reality the electron cannot ride on just a single soliton from donor to acceptor. Several solitons should be involved in transport. We have already mentioned this kind of promiscuity of the electron. Therefore the above given soliton velocity is an upper bound for the ET process. In principle this effect may be used as a way to manipulate the transfer of electrons between donor and acceptor. Clearly in our case we may have a polaron effect due to the electron–phonon (or soliton) interaction in addition to the genuinely lattice soliton effect due to the anharmonicity of the lattice vibrations. Thus, from *donor* to *acceptor*, we have not just phonon-assisted ET but a much faster soliton-assisted ET.

4.3 Adiabatic Canonical Distributions in the Tight-Binding Approximation

In a first approximation with non-interacting electrons the canonical equilibrium distribution is

$$p_n^0 = \exp[\beta(\mu - E_n)], \tag{34}$$

where the chemical potential μ is given by the normalization. In the adiabatic approximation we assume that this distribution is reached in a very short time. Using the approximation (Eq. (28)) we get

$$p_n^0 \simeq \exp\left[-\frac{\delta E_n}{k_B T}\right] = \exp\left[-\frac{\chi(q_{n+1} - q_{n-1})}{B k_B T}\right]. \tag{35}$$

Suppose now that one big soliton is excited by appropriate heating of the lattice to the temperature T. We assume the following shape of the solution

$$\exp[-3(q_n - q_{n-1}) = 1 + \beta_0 \cosh^{-1}[\kappa n - \beta_0 t]. \tag{36}$$

Incidentally, the computations by Rice and collaborators [71, 72] show that for Morse or L-J [L-J(12-6) and L-J(32-6)] potentials a Gaussian profile could also be used as an reasonably valid approximation to the exact solution (Eq. (36)) of the Toda lattice.

By introducing this into Eq. (35) we find

$$p_n^0 \simeq [1 + \beta_0 \cosh^{-2}[\kappa n - \beta_0 t]]^{\zeta} [1 + \beta_0 \cosh^{-2}[\kappa(n+1) - \beta_0 t]]^{\zeta}, \tag{37}$$

where

$$\zeta = \frac{\chi}{6 B k_B T}. \tag{38}$$

We see that a thermally excited soliton is quite similar to a mechanically excited soliton except for some kind of a twin structure and a little deformation of the shape and the amplitude, both temperature-dependent. The velocity of such thermal soliton is the same as the standard soliton velocity.

Quantum mechanically the canonical equilibrium distribution is given by the time-dependent energy eigenvalues and hence rather than Eq. (35) we now get

$$p_n^0 \simeq \exp[-c(q_{n+1}(t) - q_{n-1}(t))], \tag{39}$$

with $c = \chi / B k_B T$. The displacements have to be taken from computer simulations of thermally excited solitons. The distribution is a quickly changing local function of the displacements. In the *adiabatic* approximation we assume that this distribution is reached in a very short time, as shown in Fig. 10. Noteworthy is that this picture of a canonical quantum distribution is qualitatively similar to the classical distributions shown in Fig. 5. We may estimate the soliton frequency from the thermal statistics

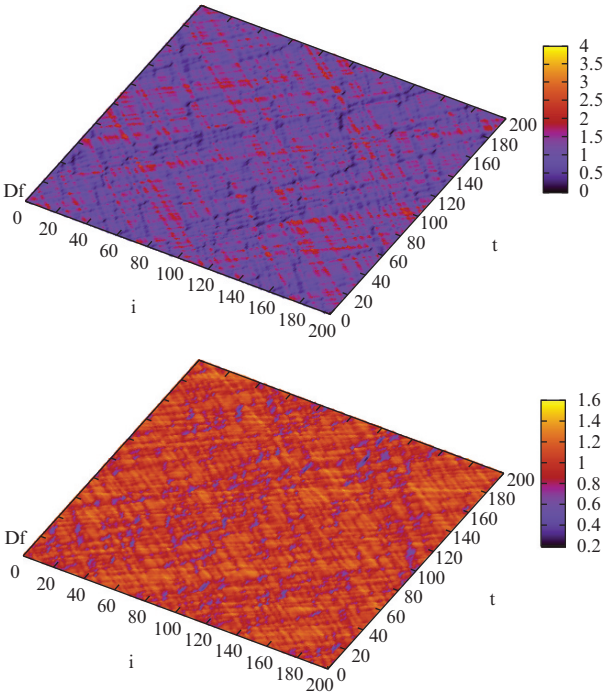

Fig. 10 Toda–Morse lattice. Probability distribution of an electron in a heated anharmonic lattice in the *adiabatic* approximation according to the quantum canonical distribution. The actual time evolution of the distribution is displayed. Upper figure: $T = 0.1$; lower figure: $T = 0.5$. Parameter values: $B\sigma = 1$, $\alpha = 1.75$, $V_0 = 1$, $\tau = 10$ and $\gamma = 0.002$

of the solitons in the lattice as done in Refs. [70, 73] for Toda interactions: (i) single solitons with parameter κ are described by Eq. (36); and (ii) the density of solitons depending on parameter κ is known. Following [73] we have

$$n(\kappa, T) = \frac{4a\kappa}{\pi k_B T} \exp(-\kappa) \exp[-(E(\kappa) - 2\kappa)/k_B T], \tag{40}$$

where

$$E(\kappa) = \frac{2a}{b}[\sinh \cosh \kappa - \kappa]. \tag{41}$$

Since the quantities p_n depend on κ we get this way the distribution of electron occupation numbers. In a thermally excited system, the number of solitons depends on the initial and boundary conditions. In an infinite Toda system (and the like for a Morse potential) the number of solitons can be approximated by

$$n(T) \simeq const\, T^{1/3}. \tag{42}$$

Thus the number of solitons appears increasing with increasing temperature. On the other hand their contribution to macroscopic properties, as, e.g. the specific heat goes down as seen in Fig. 2. Therefore we expect that there exists a kind of "optimal temperature" where solitons have the strongest influence [70, 81].

5 Coulomb Repulsion and Electron-Lattice Dynamics in Hubbard Approximation

Let us complete our analysis by considering in more details the role of Coulomb repulsion between two added excess electrons thus supplementing our findings in Sections 3.3. and 3.4. We shall do it in the simplest possible way using Hubbard's model Hamiltonian [102–104]. Thus shall take the Coulomb repulsion when the electrons are at their shortest separation distance (local on-site repulsion).

5.1 The Hubbard Hamiltonian

When we add a spin variable and augment (Eq. (24)) with an on-site local (Coulomb)–Hubbard repulsion we get

$$H_{el} = -\sum_{n,\sigma} \left(V_{n\,n-1}\, \hat{a}^{+}_{n\sigma} \hat{a}_{n-1\sigma} + V_{n\,n+1} \hat{a}^{+}_{n\sigma} \hat{a}_{n+1\sigma} \right) + U \sum_{n} \hat{a}^{+}_{n\uparrow} \hat{a}_{n\uparrow} \hat{a}^{+}_{n\downarrow} \hat{a}_{n\downarrow} \,, \quad (43)$$

where the index n denotes the lattice site. Here σ accounts for the electron spin which can be up or down. For clarity we now have made explicit the Fermion operators $\hat{a}^{+}_{n\sigma}$ creates an electron with spin σ at site n and $\hat{a}_{n\sigma}$ annihilates the electron. The second term in Eq. (43) represents the on-site electron–electron interaction due to Coulomb repulsion of strength U (here it has positive values only). The transfer matrix is like Eq. (25). For $H_{lattice}$ we take Eq. (1) with Eq. (2).

5.2 Localized Paired Electron-Lattice Deformation States

We start with the exact two-electron wavefunction given by

$$|\psi(t)\rangle = \sum_{m,n} \phi_{mn}\left(\{p_m\}, \{q_m\}\right) \hat{a}^{+}_{m\uparrow} \hat{a}^{+}_{n\downarrow} |0\rangle \,, \quad (44)$$

where $|0\rangle$ is the vacuum state (containing no electrons) and ϕ_{mn} denotes the probability amplitude for an electron with spin up to occupy site m while an electron

with spin down is at site n; $p_n = mv_n$. The symmetric $\phi_{mn} = \phi_{nm}$ probability amplitudes are normalized $\sum_{mn} |\phi_{mn}|^2 = 1$ and depend on the set of lattice variables $(\{p_n\}, \{q_n\})$.

To obtain the equations of motion for the probability amplitudes the wavefunction (Eq. (44)) is inserted into the corresponding Schrödinger equation and the evolution of the lattice variables is derived from Hamilton's variational principle with an energy functional $\mathcal{E}^2 = \langle\psi|H|\psi\rangle$. Suitable choice of scales permits rewriting the evolution equations in dimensionless form in a similar way as earlier done. Then we get:

$$\begin{aligned} i\,\frac{d\phi_{mn}}{dt} = &-\tau\,\{\exp[-\alpha\,(q_{m+1}-q_m)\,]\,\phi_{m+1n} + \exp[-\alpha\,(q_m-q_{m-1})\,]\,\phi_{m-1n} \\ &+ \exp[-\alpha\,(q_{n+1}-q_n)\,]\,\phi_{mn+1} + \exp[-\alpha\,(q_n-q_{n-1})\,]\,\phi_{mn-1}\,\} \\ &+\bar{U}\,\phi_{mn}\delta_{mn}, \end{aligned} \tag{45}$$

$$\begin{aligned} \frac{d^2q_n}{dt^2} = &\,[1-\exp\{-(q_{n+1}-q_n)\,\}]\exp[-(q_{n+1}-q_n)\,] \\ &-[1-\exp\{-(q_n-q_{n-1})\,\}]\,\exp[-(q_n-q_{n-1})\,] \\ &+\alpha V\exp[-\alpha\,(q_{n+1}-q_n)\,] \\ &\sum_m \left\{\,[\phi^*_{mn+1}\phi_{mn}+\phi^*_{mn}\phi_{mn+1}]+[\phi^*_{n+1m}\phi_{nm}+\phi^*_{nm}\phi_{n+1m}]\,\right\} \\ &-\alpha V\exp[-\alpha\,(q_n-q_{n-1})\,] \\ &\sum_m \left\{\,[\phi^*_{mn}\phi_{mn-1}+\phi^*_{mn-1}\phi_{mn}]+[\phi^*_{nm}\phi_{n-1m}+\phi^*_{n-1m}\phi_{nm}]\,\right\}. \end{aligned} \tag{46}$$

Comparing with the equations in Section 4, Eq. (45) replaces Eq. (32), having assumed, for simplicity, that all on-site diagonal factors are equal and hence can be scaled away by suitable choice of the reference energy level. This suffices for our purpose in this Section. Correspondingly, Eq. (46) replaces Eq. (33). As in Eqs. (32) and (33) the parameter τ appearing in the R.H.S. of Eq. (45) determines the degree of time scale separation between the (fast) electronic and (slow) acoustic phonon or soliton processes. For computational illustration we shall use in what follows: $\tau = 10$, $V = 0.1$, and $\alpha = 1.75$. To obtain localized stationary solutions of the coupled system (Eqs. (45) and (46)) an energy functional is minimized yielding the lowest energy configuration.

The probability for one electron to be in site n with spin up, respectively spin down, is determined by

$$\rho_{n\uparrow} = \langle\psi|\hat{a}^+_{n\uparrow}\hat{a}_{n\uparrow}|\psi\rangle = \sum_k |\phi_{nk}|^2\,, \tag{47}$$

$$\rho_{n\downarrow} = \langle\psi|\hat{a}^+_{n\downarrow}\hat{a}_{n\downarrow}|\psi\rangle = \sum_k |\phi_{kn}|^2\,. \tag{48}$$

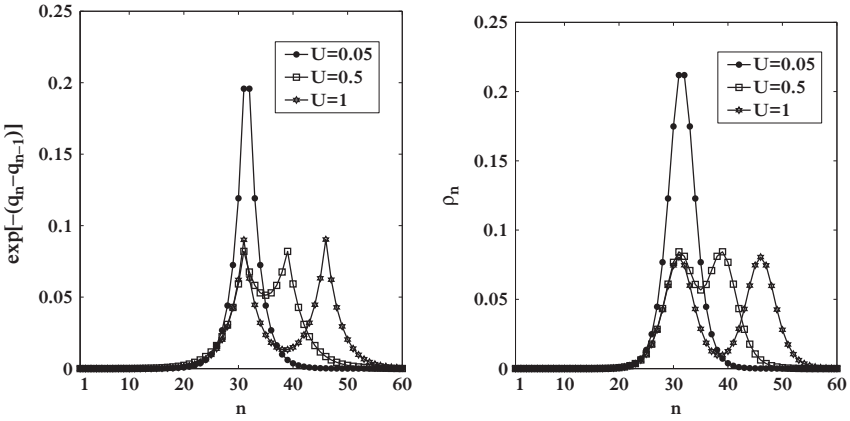

Fig. 11 Toda–Morse lattice. Lattice solitons and the role of Coulomb repulsion for an electron pair. Left figure: initial profile of the localized lattice deformation; right figure: electron probability distribution corresponding to a minimum of the variational energy for three different values of the Hubbard parameter U (values in insets). Other parameter values: $\alpha = 1.75$ and $V = 0.1$

Typical electron probability distributions and the corresponding profile of displacements of the molecules are depicted in Fig. 11 for three different values of U (because of symmetry $\rho_{n\uparrow} = \rho_{n\downarrow}$ and we plot half the electron density at a site n defined as $\rho_n = \frac{1}{2}\sum_k (|\phi_{kn}|^2 + |\phi_{nk}|^2)$). The corresponding localized compound comprises an exponentially localized two-electron state and the associated pair of kink-shape lattice deformations which represented as $\exp(-(q_n - q_{n-1}))$ are of bell-shape. These are the earlier introduced lattice solitons (Eq. (36)). Increasing the repulsive (Coulomb–) Hubbard-interaction has the impact that the inter-electron distance (and accordingly also the distance between the centers of the solitons) widens. At the same time the degree of localization reduces, i.e. broader profiles of lower peak values result. Notably, the localized solutions are fairly broad width and thus are expected to be mobile when appropriate kinetic energy is added. While for low values $U \lesssim 0.05$ the electron probability density is single-peaked increasing U causes a split up of ρ_n into a double-peak structure. For $U \gtrsim 0.9$ the inter-electron distance exceeds the width of either of the two peaks of the electron probability density. Therefore the two electrons can no longer be regarded as paired. Those features of the electron probability are equivalently exhibited by the soliton patterns, that is the stronger the repulsive interaction is, the less is the lattice compression reflected in the width and amplitude of the soliton patterns.

5.3 Moving Electron-Pair Soliton Compounds

Let us now see the evolution of the localized electrons coupled with the corresponding lattice deformations. The motion of the lattice soliton is achieved with the excitation of the soliton momenta according to

$$
\begin{aligned}
p_n = 2\sinh(\kappa)/\kappa \,\{&\exp[2\kappa(n-1)]/(1+\exp[2\kappa(n-1)]) \\
&-\exp[2\kappa(n-l)]/(1+\exp[2\kappa\,(n-l)])\} \\
+2\sinh(\kappa)/\kappa \,\{&\exp[2\kappa(n-l-1)]/(1+\exp[2\kappa(n-l-1)]) \\
&-\exp[2\kappa(n-l)]/(1+\exp[2\kappa\,(n-l)])\}\,. \qquad (49)
\end{aligned}
$$

One should bear in mind that while in this way the lattice is equipped with kinetic energy the electrons are presented as a standing state. To investigate whether a soliton-assisted transport is achievable for two correlated standing electrons in the lattice suffices to integrate the system (Eqs. (45) and (46)). For illustration this has been done with $N = 61$ lattice sites and as in all previous cases with periodic boundary conditions. The evolution of paired electrons and solitons for repulsive interaction strength, $U = 0.05$, is illustrated in Fig. 12. Noteworthy is that for such

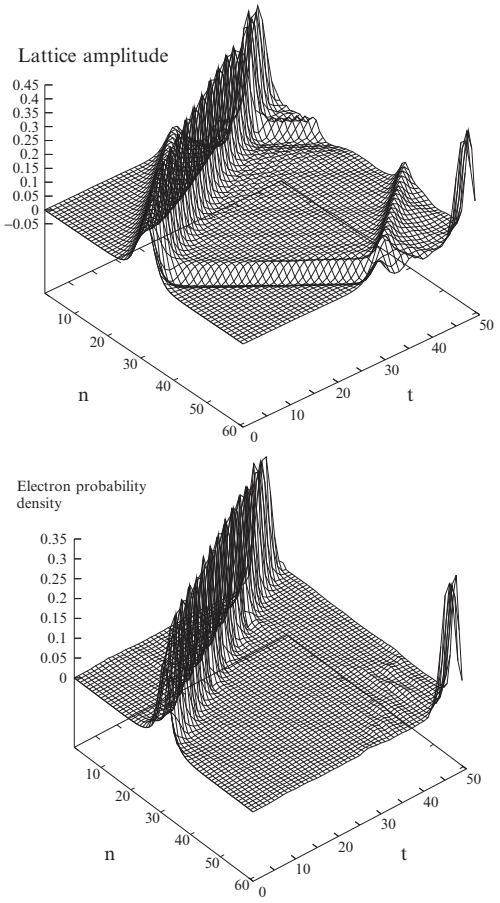

Fig. 12 Toda–Morse lattice. Upper figure: spatio-temporal evolution of a lattice soliton pair; and bottom figure: the electron probability distribution. Parameter values: $\alpha = 1.75$, $V = 0.1$ and $U = 0.05$

particular values the lattice solitons travel with *subsonic* velocity along the lattice retaining their localized profile save an early emission of small radiation to either side. Likewise the localized shape of the electron pair probability distribution as well as the inter-electron distance of a single site are maintained throughout the computation. Apparently part of the energy contained initially in the lattice deformation flows to the electronic degree of freedom with the result that the height of the electron probability density increases, with consequent lowering of the velocity of the corresponding solitons. For higher repulsion strengths, $U \gg 0.05$, *supersonic* moving paired electron lattice solitons compounds can be observed as it is the case for $\alpha = 2$ and $V = 0.25$ for which an inter-electron distance of a single site is attained.

6 Summary and Concluding Remarks

Davydov's approach to ET in biomolecules was a clever combination of physical insight and mathematical beauty. His electro-soliton concept was a fruitful step forward from the polaron concept due to Landau and Pekar. In both cases the underlying lattice dynamics is *harmonic* hence leading to phonons which are linear, infinitesimal excitations of the lattice crystal. The electro-soliton originates in the nonlinearity of the electron–lattice coupling. A natural generalization of the polaron and electro-soliton concepts is possible if consideration of lattice *anharmonicity* is added to the electron–lattice interaction. Indeed, if we focus first on the anharmonic lattice dynamics there are known Hamiltonian cases like the Toda one which being integrable possess as exact solutions, both solitons and solitonic periodic waves obtained in analytical compact form. Such lattice solitons are natural "carriers" of either matter or charge along the lattice crystal [105] and can trap excess, added electrons thus leading to dynamic bound states which have been called solectrons. There is a major component in the solectron concept that makes clear-cut distance with Davydov's electro-soliton. The underlying lattice excitations are of finite amplitude, and not merely infinitesimal.

Davydov's electro-solitons do not survive above 10 K and do this with just a few picoseconds lifetimes. In the present report we have shown that at variance with Davydov's electro-solitons, at least for Morse–Toda-like interactions thermally excited solectrons survive well above the physiological or room temperature range (ca. 300 K) with several picoseconds lifetimes. First we have shown that thermally excited solitons do survive at such temperatures. This was explored assuming that lattice units are atoms or screened ion cores and then tracking lattice compressions by the alternative offered by enhanced (covalent) electron densities. Then adding excess, free (conduction) electrons we have shown how solectrons are formed and survive at the physiological or room temperature range. Subsequently, we have considered pairs of electrons with added Coulomb repulsion albeit in the local, screened Hubbard approximation. The computer simulations have shown that electron pairs dynamically bound to solitons can travel along the charged lattice with speeds either

subsonic or supersonic. It clearly appears that Coulomb repulsion does not alter the possibility of solectrons being ET carriers or at the origin of a new form of (non-Ohmic) electric conduction in the presence of an external field [75]. Furthermore, by allowing electron pairing the results here reported open the path to the study of solectron pairs as Bosons and whether or not such a system is prone to Bose–Einstein condensation is an appealing question.

Acknowledgements The authors are grateful to Professors J.J. Kozak, G. Nicolis and G. Tsironis, for fruitful discussions. This research has been sponsored by the EU under Grant SPARK II-FP7-ICT-216227 and by the Spanish Government under Grant MEC-VEVES-FIS2006-01305.

References

1. B. Alberts, D. Bray, J. Lewis, M.Raff, K. Roberts, J.D. Watson, *Molecular Biology of the Cell* (Garland, New York, 1983)
2. J.A. McCammon and S.C. Harvey, *Dynamics of Proteins and Nucleic Acids* (Cambridge University Press, Cambridge, 1987)
3. C. Branden and J. Tooze, *Introduction to Protein Structure* (Garland, New York, 1991)
4. J.J. Hopfield, Proc. Nat. Acad. Sci. USA **71**, 3649 (1974)
5. D.N. Beratan, J.N. Onuchic, J.J. Hopfield, J. Chem. Phys. **86**, 4488 (1987)
6. J.J. Hopfield, J.N. Onuchic, D.N. Beratan, Science **241**, 817 (1988)
7. J.N. Onuchic and D.N. Beratan, J. Chem. Phys. **92**, 722 (1990)
8. D.N. Beratan, J.N. Betts, J.N. Onuchic, Science **252**, 1285 (1991)
9. J.N. Onuchic, P.C.P. Andrade, D.N. Beratan, J. Chem. Phys. **95**, 1131 (1991)
10. K. Schulten, M. Tesh, Chem. Phys. **158**, 421 (1991)
11. J.N. Onuchic, D.N. Beratan, J.R. Winkler, H.B. Gray, A. Rev. Biophys. Struct. **21**, 349 (1992)
12. C. Turrò, C.K. Chang, G.E. Leroi, R.I. Cukier, D.G. Nocera, J. Am. Chem. Soc. **114**, 4013 (1992)
13. M.H. Vos, M.R. Jones, C.N. Hunter, J. Breton, J.-C. Lambry, J.-L. Martin, Biochem. **33**, 6759 (1994)
14. H.B. Gray, J.R. Winkler, Annu. Rev. Biochem. **65**, 537 (1996)
15. S.S. Skourtis, D.N. Beratan, J. Biol. Inorg. Chem. **2**, 378 (1997)
16. M. Bixon, B. Giese, S. Wessely, T. Langenbacher, M.E. Michel-Beyerle, J. Jortner, Proc. Natl. Acad. Sci. USA **96**, 11713 (1999)
17. V. Sartor, P.T. Henderson, G.B. Schuster, J. Am. Chem. Soc. **121**, 11027 (1999)
18. C. Wan, T. Fiebig, S.O. Kelley, C.R. Treadway, J.K. Barton, A.H. Zewail, Proc. Natl. Acad. Sci. USA **96**, 6014 (1999)
19. E.M. Conwell, S.V. Rakhmanova, Proc. Natl. Acad. Sci. USA **97**, 4556 (2000)
20. E.W. Schlag, D.-Y. Yang, S.-Y. Sheu, H.L. Selzle, S.H. Lin, P.M. Rentzepis, Proc. Natl. Acad. Sci. USA **97**, 9849 (2000)
21. C. Wan, T. Fiebig, O. Schiemann, J.K. Barton, A.H. Zewail, Proc. Natl. Acad. Sci. USA **97**, 14052 (2000)
22. S.-Y. Sheu, D.-Y. Yang, H.L. Selzle, E.W. Schlag, Eur. Phys. J. D **20**, 557 (2002)
23. H.B. Gray, J.R. Winkler, Proc. Natl. Acad. Sci. USA **102**, 3534 (2005)
24. L.D. Landau, Phys. Z. Sowjetunion **3**, 664 (1933)
25. S.I. Pekar, Sov. Phys. JETP, **16**, 335 (1946)
26. L.D. Landau, S.I. Pekar, Sov. Phys. JETP, **18** 419 (1948)
27. T.D. Holstein, Ann. Phys. NY **8**, 325, 343 (1959)
28. A.S. Alexandrov, N. Mott *Polarons and Bipolarons*, (World Scientific, Singapore 1995)
29. A.S. Davydov, J. Theor. Biol. **38**, 559 (1973)

30. A.S. Davydov, N.I. Kislukha, Sov. Phys. JETP **44**, 571 (1976)
31. A. S. Davydov, Sov. Phys. Rev. B **25**, 898 (1982)
32. A.S. Davydov, *Solitons in Molecular Systems*, 2nd edn. (Reidel, Dordrecht, 1991)
33. A.L. Christiansen, A.C. Scott (eds.), *Davydov's Soliton Revisited. Self-Trapping of Vibrational Energy in Protein* (Plenum Press, New York, 1983)
34. A.C. Scott, Phys. Rep. **217**, 1 (1992)
35. M. Peyrard (ed.), *Nonlinear Excitations in Biomolecules* (Springer-Verlag, Berlin, 1995)
36. P.S. Lomdahl, W.C. Kerr, Phys. Rev. Lett. **55**, 1235 (1985)
37. H. Fröhlich, Proc. R. Soc. London, Ser. A **215**, 291 (1952)
38. H. Fröhlich, Phys. Lett. **26A**, 402 (1968)
39. H. Fröhlich, Int. J. Quant. Chem. **2**, 641 (1968)
40. H. Fröhlich, Nature (London) **228**, 1093 (1970)
41. H. Fröhlich, Phys. Lett. **39A**, 153 (1972)
42. H. Fröhlich, Phys. Lett. **51A**, 21 (1975)
43. H. Fröhlich, Nuovo Cimento **7**, 416 (1977)
44. J.A. Tuszynski, R. Paul, R. Chatterjee, S.R. Sreenivasan, Phys. Rev. A **30**, 2666 (1984)
45. O.H. Olsen, M.R. Samuelsen, S.B. Petersen, L. Nørskov, Phys. Rev. A **38**, 5856 (1988)
46. A.V. Zolotaryuk, P.L. Christiansen, A.V. Savin, Phys. Rev. E **54**, 3881 (1996)
47. P.L. Christiansen, A.V. Zolotaryuk, A.V. Savin, Phys. Rev. E **56**, 877 (1997)
48. A.V. Zolotaryuk, K.H. Spatschek, A.V. Savin, Phys. Rev. B **54**, 266 (1996)
49. S. Caspi, E. Ben-Jacob, Europhys. Lett. **47**, 522 (1999)
50. S.W. Englander, N.R. Kallenbach, A.J. Heeger, J.A. Krumhansl, S. Litwin, Proc. Nat. Acad. Sci. USA **77**, 7222 (1980)
51. M. Peyrard, A.R. Bishop, Phys. Rev. Lett. **62**, 2755 (1989)
52. G. Gaeta, C. Reiss, M. Peyrard, T. Dauxois, Riv. Nuovo Cim. **17**, 1 (1994)
53. T. Dauxois, M. Peyrard, *Physics of Solitons* (Cambridge University Press, Cambridge, 2006)
54. A.C. Scott, *The Nonlinear Universe. Chaos, Emergence, Life* (Springer, Berlin, 2007)
55. Q. Xie, G. Archontis, S.S. Skourtis, Chem. Phys. Lett. **312**, 237 (1999)
56. E.S. Medvedev, A.A. Stuchebrukhov, J. Chem. Phys. **107**, 3821 (1997)
57. S. Yomosa, Phys. Rev. A **32**, 1752 (1985)
58. D. Hennig, Phys. Rev. E **64**, 041908 (2001)
59. N. Voulgarakis, D. Hennig, H. Gabriel, G.P. Tsironis, J. Phys.: Cond. Matter **13**, 9821 (2001)
60. D. Hennig, Eur. Phys. J. B **24**, 377 (2001)
61. D. Hennig, Phys. Rev. B **65**, 174302 (2002)
62. D. Hennig, Physica A **309**, 243 (2002)
63. D. Hennig, Eur. Phys. J. B **30**, 211 (2002)
64. S. Komarnicki, D. Hennig, J. Phys.: Cond. Matter **15**, 441 (2002)
65. D. Hennig, J.F.R. Archilla, J. Agarwal, Physica D **180**, 256 (2003)
66. M. Toda, *Theory of Nonlinear Lattices*, 2nd edn. (Springer-Verlag, New York, 1989) (and references therein)
67. T.P. Valkering, J. Phys. A: Math. Gen. **11**, 1885 (1978)
68. G. Friesecke, J.A.D. Wattis, Commun. Math. Phys. **161**, 391 (1994)
69. V.I. Nekorkin, M.G. Velarde, *Synergetic Phenomena in Active Lattices. Patterns, Waves, Solitons, Chaos* (Springer-Verlag, Berlin, 2002)
70. F.G. Mertens, H. Büttner, in *Solitons*, edited by S.E. Trullinger, V.E. Zakharov and V.L. Pokrousky (North-Holland, Amsterdam, 1986) ch. 15
71. J. Dancz, S.A. Rice, J. Chem. Phys. **67**, 1418 (1977)
72. T.J. Rolfe, S.A. Rice, J. Dancz, J. Chem. Phys. **70**, 26 (1979)
73. F. Marchesoni, C. Lucheroni, Phys. Rev. B **44**, 5303 (1991)
74. A.P. Chetverikov, W. Ebeling, M.G. Velarde, Eur. Phys. J. B **44**, 509 (2005)
75. M.G. Velarde, W. Ebeling, A.P. Chetverikov, Int. J. Bifurcation Chaos **15**, 245 (2005)
76. A.P. Chetverikov, W. Ebeling, M.G. Velarde, Eur. Phys. J. B **51**, 87 (2006)
77. A.P. Chetverikov, W. Ebeling, M.G. Velarde, Int. J. Bifurcation Chaos **16**, 1613 (2006)
78. V.A. Makarov, M.G. Velarde, A.P. Chetverikov, W. Ebeling, Phys. Rev. E *73*, 066626 (2006)
79. M. G. Velarde, W. Ebeling, D. Hennig, C. Neissner, Int. J. Bifurcation Chaos **16**, 1035 (2006)

80. D. Hennig, C. Neissner, M.G. Velarde, W. Ebeling, Phys. Rev. B **73**, 024306 (2006)
81. A.P. Chetverikov, W. Ebeling, G. Röpke, M.G. Velarde, Contr. Plasma Phys. **47**, 465 (2007)
82. D. Hennig, A. Chetverikov, M.G. Velarde, W. Ebeling, Phys. Rev. E **76**, 046602 (2007)
83. M.G. Velarde, W. Ebeling, A.P. Chetverikov, D. Hennig, Int. J. Bifurcation Chaos **18**, 521 (2008)
84. P. Morse, Phys. Rev. **34**, 57 (1929)
85. M.G. Velarde, Int. J. Comput. Appl. Math. DOI 10.10.16/j.cam.2008.07.058
86. W. Ebeling, I.M. Sokolov, *Statistical Thermodynamics and Stochastic Theory of Nonequilibrium Systems* (World Scientific, Singapore, 2005)
87. G. Kalosakas, S. Aubry, G.P. Tsironis, Phys. Rev. B **58**, 3094 (1998)
88. G. Kalosakas, K.O. Rasmussen, A.R. Bishop, J. Chem. Phys. **118**, 3731 (2003)
89. G. Kalosakas, K.O. Rasmussen, A.R. Bishop, Synthetic Metals **141**, 93 (2004)
90. V. Heine, D. Weaire, Pseudopotential Theory of Cohesion and Structure, in *Solid State Physics*, vol. 24, pp. 250–463, eds. H. Ehrenreich, F. Seitz, D. Turnbull (Academic, New York, 1970)
91. W.D. Kraeft, D. Kremp, W. Ebeling, G. Röpke, *Quantum Statistics of Charged Particle Systems* (Akademie-Verlag, Berlin, 1986)
92. J.S. Blakemore, *Semiconductor Statistics* (Pergamon Press, 1962); *Solid State Physics* (Cambridge University Press, Cambridge, 1985)
93. W.A. Harrison, *Solid State Theory* (Dover Ed., New York, 1979)
94. P.W. Anderson, Phys. Rev. **112**, 1900 (1958)
95. I.M. Lifshitz, S.A. Gredeskul, L.A. Pastur, *Introduction to the Theory of Disordered Systems* (in Russian) (Nauka, Moscow, 1982)
96. V.A. Schweigert, F.M. Peeters, Phys. Rev. B **51**, 7700 (1995)
97. V.M. Bedanov, F.M. Peeters, Phys. Rev. B **49**, 2667 (1994)
98. M. Bonitz, V. Golubichnyi, A.V. Filinov, Yu.F. Lozovik, Microelectron. Eng. **62**, 141 (2002)
99. M. G. Velarde, C. Neissner, Int. J. Bifurcation Chaos **18**, 885 (2008)
100. J.D. Patterson, B.C. Bailey, *Solid State Physics. Introduction to the Theory* (Springer-Verlag, Berlin, 2007)
101. H. Böttger, V.V. Bryksin, *Hoping Conduction in Solids* (Academie-Verlag, Berlin, 1985)
102. J. Hubbard, Proc. Roy. Soc. (London) A **276**, 238 (1963); A **277**, 237 (1964); A **281**, 401 (1964)
103. A. Montorsi (ed.), *The Hubbard Model. A Reprint Volume* (World Scientific, Singapore, 1992)
104. D. Hennig, M.G. Velarde, W. Ebeling, A.P. Chetverikov, Phys. Rev. E, **78**, 066606 (2008)
105. E. del Rio, M.G. Velarde, W. Ebeling, Physica A **377**, 435 (2007)